THE RELATIONSHIP BETWEEN CORONAL DIMMING AND CORONAL MASS EJECTION PROPERTIES

A. A. REINARD[1,3] AND D. A. BIESECKER[2]

[1] University of Colorado/Cooperative Institute for Research in Environmental Sciences and National Oceanic and Atmospheric Administration/Space Weather Prediction Center, Boulder, CO, USA; alysha.reinard@noaa.gov

[2] National Oceanic and Atmospheric Administration/Space Weather Prediction Center, Boulder, CO, USA

ABSTRACT

Coronal dimmings are closely related to the footpoints of coronal mass ejections (CMEs) and, as such, offer information about CME origins and evolution. In this paper, we investigate the relationship between CME and dimming properties. In particular, we compare CME quantities for events with and without associated dimmings. We find that dimming-associated CMEs, on average, have much higher speeds than non-dimming-associated events. In fact, CMEs without an associated dimming do not appear to travel faster than 800 km s^{-1}, i.e., the fast solar wind speed. Dimming-associated events are also more likely to be associated with flares, and those flares tend to have the highest magnitudes. We propose that each of these phenomena is affected by the energy available in the source region. Highly energetic source regions produce fast CMEs that are accompanied by larger flares and visible dimmings, while less energetic source regions produce slow CMEs that are accompanied by smaller flares and may or may not have dimmings. The production of dimmings in the latter case may depend on a number of factors including initiation height of the CME, source region magnetic configuration, and observational effects. These results have important implications for understanding and predicting CME initiations.

Key words: Sun: activity – Sun: corona – Sun: coronal mass ejections (CMEs)

1. INTRODUCTION

Coronal dimmings, also called transient coronal holes or depletions, are regions in the low corona consisting of reduced emission in white light, extreme ultraviolet (EUV), and soft X-rays (Hansen et al. 1974 ; Rust & Hildner 1976; Sterling & Hudson 1997; Thompson et al. 1999, 2000a; Gopalswamy & Hanaoka 1998). Dimmings are often seen during the early phase of a CME and are interpreted as a mass depletion due to the loss or rapid expansion of the overlying corona (Hudson et al. 1998; Harrison & Lyons 2000; Harra & Sterling 2001; Harra et al. 2007). The disappearance of the "moss" (Berger et al. 1999) pattern during the dimming formation is interpreted as a sign of the opening of the coronal magnetic field (McIntosh et al. 2007), supporting the idea of outflow in dimming regions.

As one of the clearest on-disk signatures, coronal dimmings offer a unique view into the evolution of the coronal magnetic structure during and after the eruption. Comparisons between dimmings and CME properties can provide important insight into CME evolution. Dimming areas appear closely aligned with the apparent footpoint of the white-light CME (Thompson et al. 2000b, Harrison et al. 2003). Dimming sizes can vary from compact (∼ size of an active region) to widespread (covering the solar disk) but typically span a much larger area than the flare, while dimming durations vary between a few hours to two days or longer (Reinard & Biesecker 2008). These observations suggest that magnetic reconfiguration of CME footpoints occurs on a large scale, and the effects remain long after the CME has left the corona. The study of dimmings has the potential to directly affect our understanding of CME dynamics, and may have further implications for resulting CME and interplanetary coronal mass ejection (ICME) properties.

In a study of 114 halo CMEs, Reinard & Biesecker (2008) found only 30 had detectable dimmings associated with them. Since we would expect half of these halo CMEs to be directed Earthward, we infer that visible dimmings are present for

30/57 (53%) of these Earth-directed halo CMEs. This result raises the important question: what is the difference between CMEs with associated dimmings and those without? In this paper, we look at CME properties in the context of associated dimming properties to determine if there are physical properties that can be used to distinguish whether a certain type of event is more likely to be associated with a dimming.

2. METHOD

The motivation for this study is to use dimmings to better understand the processes involved in the early evolution of CMEs. In this paper, we focus on CME (i.e., near-Sun) quantities to determine what properties distinguish CMEs with large dimmings from those with small/no dimmings. A companion paper (A. A. Reinard et al. 2009, in preparation) will use the same events to investigate associations between dimmings and ICME quantities. The events that were chosen for these two studies have both in situ and solar CME observations.

We use the lists by Richardson & Cane (2008) and Qiu et al. (2007) to determine CME–ICME associations. For each CME observation, *Solar and Heliospheric Observatory* (*SOHO*) Extreme-ultraviolet Imaging Telescope (EIT) fixed-difference images were inspected to determine whether or not a dimming was present. Cases for which the dimming association was unclear or impossible to determine were removed from the study. Observations extended from 1997 through 2005, covering nearly an entire solar cycle. We find 90 CMEs for which we could determine unambiguously whether or not a dimming was present. Of these 90 events, 65 had associated dimmings and 25 did not. Note that these values should not be taken to indicate what percentage of CMEs are associated with dimmings because in this effort we used very strict criteria and removed all events which were deemed to be doubtful, a determination that affects the non-dimming-associated events more than the dimming-associated events. We also note that in some cases dimmings may be present but unseen due to the sensitivity level of EIT (Bewsher et al. 2008). Therefore, the wording "non-dimming-

---

[3] NOAA/SPWC, 325 S Broadway St Boulder, CO 80505.
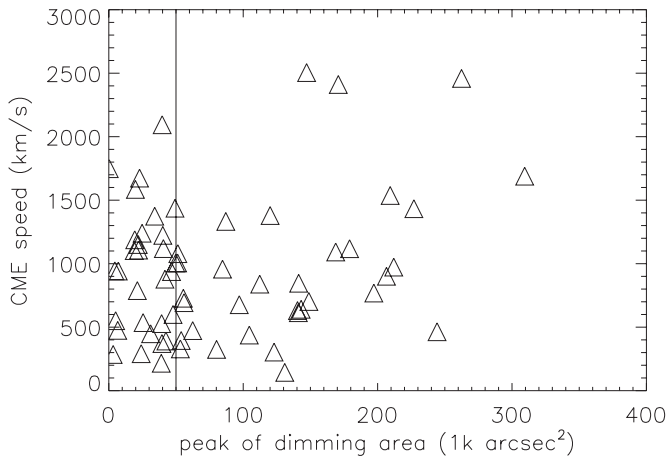
Figure 1. Peak dimming area vs. CME velocity (km s^{-1}). A very weak association is present with the largest dimmings being more likely to occur with faster CMEs.

Figure 2. CME velocity vs. source heliolongitude based on flare location. Dimming-associated events are closed diamonds, while non-dimming-associated events are shown as open diamonds. Non-dimming-associated events do not reach speeds above 800 km s^{-1}, while dimming-associated events are present at all speeds. There is no apparent dependence on source heliolongitude.

associated CME" in the text below should be taken to indicate that no *detectable* dimming was present.

Each dimming was analyzed using the method developed in Reinard & Biesecker ([2008](#)), which provides basic measurements of the dimming area, intensity, and duration for each event. A pre-event image is determined and subtracted from each image within the event. A region of interest is selected and followed in time to determine the area (i.e., the number of pixels falling more than 1σ below the image mean) and intensity (i.e., the sum of those dim pixels) of dimmings. Each image has been corrected for solar rotation using a mapping technique, drot_map.pro, within Solarsoft (Freeland & Handy [1998](#)) that is based on the solar differential rotation formula of Howard et al. ([1990](#)). Several of the events in this study were present in Reinard & Biesecker ([2008](#)), and the additional events have been analyzed using the same method.

Associated flares and active regions were identified when present in order to include flare and active region properties in the comparison. Speed measurements are obtained from the LASCO CME Catalog (Yashiro et al. [2004](#)). Cataloged linear speed is determined by fitting a linear first-order polynomial through the measured CME height–time plot. We note that in this catalog measurements are based on the assumption of sky plane projection, which can be significant for the Earth-directed events studied here. Measurements obtained from this catalog, therefore, represent lower limits on the true unprojected values (Howard et al. [2007](#)). Events originating near the central meridian of the Sun will have the largest projection effects and thus the lowest apparent speed for a given true speed. On the other hand, these same events offer the best viewing conditions for observing dimmings. Most of our events occurred near the disk center, and (as we will show) there was no dependence on source longitude in our results, so we do not correct for projection effects. The surface area corresponding to a given area on the image can vary depending on the distance between the *SOHO* spacecraft and the Sun and for different parts of the solar disk. The former effect is a small correction, and the latter is not deemed important for this study because most of these events are halo CMEs that are centered on the solar disk.

3. RESULTS

In Figure [1](#), we compare dimming area with cataloged CME speed. There are no strong correlations in these data. However,
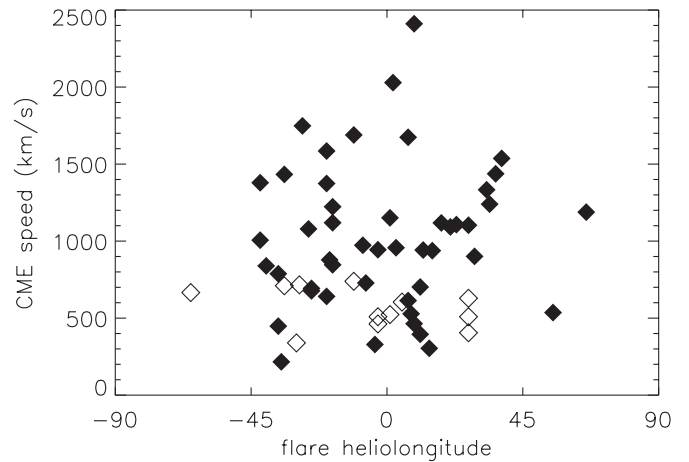
we note that, while the smallest dimmings seem to extend to all speeds, there is a positive correlation for larger dimmings. Above 50,000 arcsec^2 (indicated by the vertical lines) we see a weak correlation. For these larger events, the correlation coefficient for velocity with dimming area is 0.46 with a significance of 99.3%. This correlation coefficient reaches the level of significance, but the spread in values is very large indicating that while some association is present, the correlation is quite weak and probably due to a mutual correlation with another quantity. We have also looked at correlations between dimming area and CME acceleration and between unsigned magnetic flux within a dimming region and CME velocity/acceleration. In each case, we found no significant correlation.

It is more instructive to establish broad categories of dimming-associated and non-dimming-associated events and compare CME properties of each. In Figure [2](#), we plot CME speed versus heliolongitude of the flare. Events associated with dimming regions are given in filled diamonds and those with no associated dimmings are shown with open diamonds. The difference in CME speeds is striking. At low speeds, the dimmings and non-dimming events overlap, but at high speeds only the dimming events are present. Non-dimming-associated CMEs do not exceed a speed of 800 km s^{-1}. In fact, the highest speed reached for non-dimming events was 770 km s^{-1}. In Figure [2](#), it is also clear that there is no apparent bias or dependence on heliolongitude. Non-dimming events occur at all heliolongitudes, as do dimming events. Most events are centered within 45° of the central meridian, as expected for events with an associated in situ observation.

It is not clear from Figure [2](#) whether non-dimming events represent a separate, lower velocity population or the low-speed portion of the CME population. In Figure [3](#) (left), we plot the CME velocity in a histogram form for dimming events (black histogram) and non-dimming events (white histogram). While Figure [2](#) only includes 59 events with an associated flare, Figure [3](#) includes all the 90 events. Here we see that the non-dimming-associated events have a distribution curve nearly identical to the dimming-associated events below 800 km s^{-1}, at which point the non-dimming-associated events drop off abruptly. Dimming-associated events have a long high-speed tail that extends to 2500 km s^{-1}. On the right-hand side of Figure [3](#), we plot the total population in black and
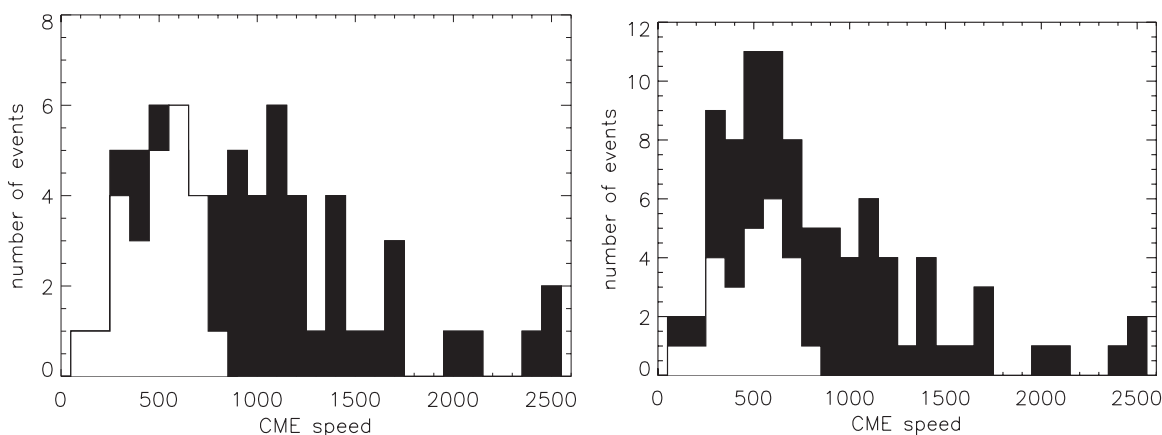
Figure 3. On the left, we plot CME speed in a histogram form with dimming-associated events in black and non-dimmings in white. The histograms are very similar for slow events, but non-dimming events cut off at approximately 800 km s^{-1}, while dimming-associated events have a much longer tail. On the right, we again plot a histogram of CME speed, but with the black representing all events. Here we can see how the non-dimming-associated events compare to the total population.
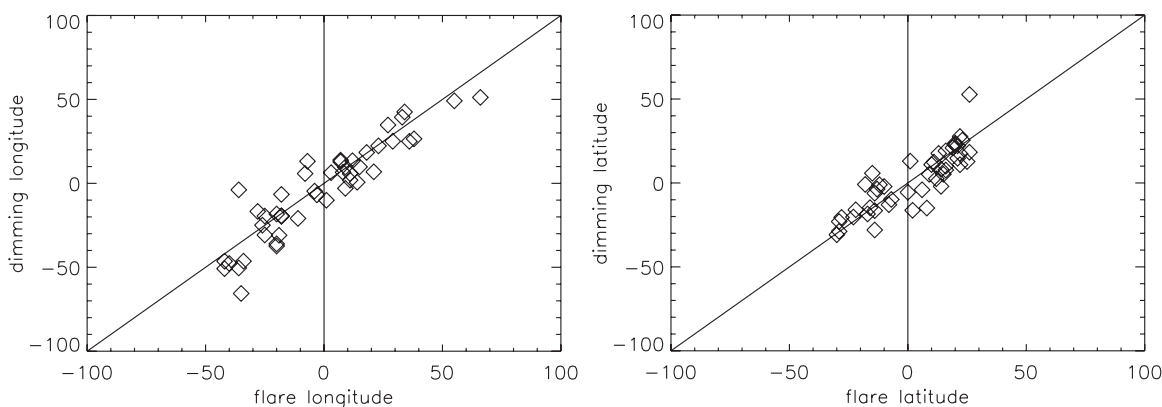
Figure 4. Dimming vs. flare longitude (left) and latitude (right). Values are similar, as expected.

non-dimming events in white. Here we see that the shape of the two distributions is quite similar with non-dimming-associated events having a truncated tail. In order to test if dimming and non-dimming events come from two different populations, we calculate the Kolmogorov–Smirnov statistic, which provides a measurement of whether two data sets are drawn from different population distribution functions (Press et al. 1989). In a comparison between dimming-associated and non-dimming-associated events, we find a value of 0.54, which indicates that the probability of the dimming and non-dimming events coming from the same population is approximately $2e^{-5}$. In other words, the CME speeds for dimming and non-dimming events represent two distinct populations.

In the above discussion, we order the data using flare heliolongitude. We do not use the dimming heliolongitude for two reasons: (1) for a consistent comparison with non-dimming events, and (2) any determination of a dimming region center is inexact because the regions are usually extended and irregular. In Figure 4, we plot the measured longitude and latitude of dimmings and flares in events where both were present and measured. A diagonal line is given to show where the points would lie if the flare and dimming positions were identical. As dimmings extend over a large region, the latitude and longitude are determined by averaging the range of values over which the dimming extends. We see that the dimming longitude (left panel) can be different than the flare longitude by as much as 30°, but typically the values are within approximately ±10°. The same is true for latitudes (right panel). The data points are

closely correlated with each other, and, thus, we are confident that we are looking at the same events in each case and that flare longitude is a reasonable proxy for the dimming location.

To determine if there is a dependence of dimming activity on the solar cycle, we plot in Figure 5 the fraction of events in each year that were fast, dimming associated; slow, dimming associated; and slow, non-dimming associated. The non-dimming-associated events occur approximately 30%–50% of the time throughout the solar cycle. The fast, dimming-associated events tend to occur most often in the declining phase of the solar cycle (2001–2006), while the slow, dimming-associated events tend to occur during the ascending phase of the solar cycle (1996–2000).

In Figure 6, we plot CME speed versus flare energy for dimming (solid diamond)- and non-dimming (open diamond)-associated events. We find that non-dimmings are generally associated with C- or M-class *GOES* X-ray flares, with the highest flare value being M8.6. Dimming-associated events appear with flares of all sizes ranging from C1.1 to X10.0. The non-dimming-associated events have a flatter slope than the dimming-associated events, with similar values in the C-class flare range, but at the low end of the velocity range for M-class flares.

In Table 1, we separate our data into two populations: average values for CMEs with associated dimming regions and for CMEs without detectable dimmings. Error bars are calculated based on $\sigma/\sqrt{n}$, where σ is the standard deviation of the population and n is the number of elements in the population. The values in the
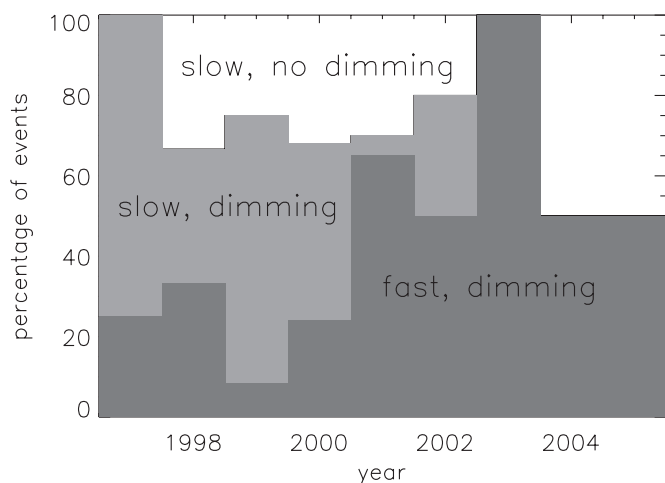
Figure 5. Solar cycle dependence. Non-dimming-associated events appear about 30%–50% of the time. Slow (<800 km s^{-1}), dimming-associated events mostly appear in the ascending phase of the solar cycle, while fast (>800 km s^{-1}), dimming-associated events dominate in the descending phase.

Figure 6. CME speed vs. flare energy. Dimming-associated events are closed diamonds, while non-dimming-associated events are shown as open diamonds. Non-dimming-associated events appear concentrated at low flare values. In the M-class flare range, the non-dimming-associated events appear to have the lowest speeds.

parenthesis indicate the number of events used to determine the average. As we see in Table 1, there is a significant difference between these two populations. Dimming-related CMEs have an average linear speed of 964 km s^{-1}, while non-dimming-associated CMEs have an average linear speed of 498 km s^{-1}. This is nearly a factor of 2 difference and well beyond the margin of error. Acceleration has no significant difference between dimming related (-5.4 km s^{-2}) and non-dimming related (0.0 km s^{-2}) events. Dimming-associated events are much more likely (72% versus 48%) to also be associated with a flare. For events with an associated flare, the flare magnitude is more than a factor of 4 higher for dimming-associated events than non-dimming-associated events (9.3 versus 1.9 e^{-5} W m^{-2}). Each of these differences is well beyond the margin of error.

At the bottom of Table 1, we subdivide dimming-associated CMEs into fast ($>=800$ km s^{-1}) and slow (<800 km s^{-1}) categories. We find that the slow, dimming-associated events have nearly the same flare association and associated flare magnitude as the non-dimming-associated events, while the fast, dimming-associated events have extremely high flare association and associated flare magnitude. In addition, we calculate the Kolmogorov–Smirnov statistic for slow dimming versus slow non-dimming populations and find a value of 0.15 indicating an 89% chance that the two populations come from the same distribution. Thus, among slow CMEs, the dimming and non-dimming events appear likely to have come from the same population.

In Table 2, we consider active region properties and divide our data into three populations: (1) dimming-associated CMEs with speeds above 800 km s^{-1}; (2) dimming-associated CMEs
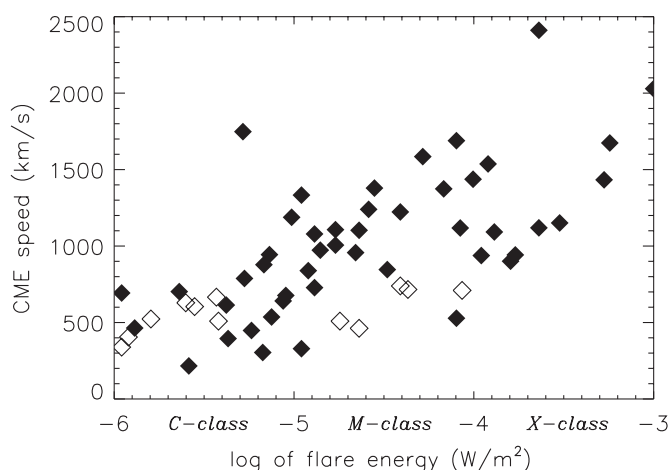
with speeds below 800 km s^{-1}; and (3) non-dimming-associated CMEs. Active region properties are taken from National Geophysical Data Center and include the active region area (in millionths of solar hemisphere), longitudinal extent (in degrees), and number of sunspots. Each of these measurements is taken approximately every six hours. These results are shown in Table 2 for the 65 events with reliable active region associations. The numbers in the parenthesis in each of the headings indicate how many events with associated active regions were present in each category. For each measurement, we select the value immediately preceding and following the event and average over all events in each population. As shown in Table 2, we find no significant change in the values of a given quantity before and after an event. The primary difference that is found between these three populations is that for each active region measurement, the fast, dimming-associated CMEs have the highest values; the slow, non-dimming-associated CMEs have values that lie in the center; and the slow, dimming-associated CMEs have the lowest values. We also looked at three quantities that measure the complexity of the active region: Zurich number, compactness, and penumbra, and found no significant difference in their values for these three populations. In addition, for all of the above active region quantities, we determine whether the values increase or decrease and whether the active regions become more complex or less complex. In each case, we find no significant, consistent differences.

4. DISCUSSION

Coronal dimmings are one of the clearest on-disk CME signatures and provide clues about the evolution of the magnetic

Table 1
CME and Flare Properties for Dimming- and Non-dimming-associated Events

CME/Flare Property	With Associated Dimming	No Detectable Dimming
CME linear speed	964 ± 69 (65)	498 ± 35 (25)
CME acceleration	-5.4 ± 5.8 (65)	0.0 ± 2.8 (25)
Flare association	47/65 (72%)	12/25 (48%)
Flare energy (1e-5 W m^{-2})	9.3 ± 2.7 (47)	1.9 ± 0.7 (12)
	Fast CMEs	Slow CMEs
Flare association	32/36 (89%)	15/29 (52%)
Flare energy (1e-5 W m^{-2})	13.2 ± 3.7	1.1 ± 0.5

Table 2
Average Active Region Properties for Different CME Speeds and Dimming Associations

Active Region Property	Fast, Dimming-associated CMEs (36)	Slow, Dimming-associated CMEs (16)	Slow, Non-dimming-associated CMEs (13)
% of events with associated AR	94%	45%	52%
Number of sunspots before event	29.5 ± 3.6	20.6 ± 3.8	24.8 ± 3.5
Number of sunspots after event	27.5 ± 3.5	23.1 ± 4.0	30.0 ± 3.5
Longitudinal extent before event	48.3 ± 11.7	11.1 ± 1.2	38.5 ± 17.6
Longitudinal extent after event	50.3 ± 11.6	10.5 ± 1.4	38.2 ± 17.8
AR area before event	422.8 ± 44.2	286.3 ± 50.0	346.2 ± 61.3
AR area after event	390.3 ± 40.7	296.9 ± 50.6	321.5 ± 48.0

structure of the CME during and after the eruption. The findings presented in this paper indicate that CMEs with associated dimmings are, on average, much faster than CMEs without associated dimmings. In addition, these events are more likely to also have associated flares and those flares tend to be larger in magnitude.

We find dimming-associated CMEs at all speeds, but non-dimming-associated CMEs do not exceed 800 km s^{-1}. The maximum value of 800 km s^{-1} for non-dimming events is interesting, as it corresponds to typical fast solar wind speeds. This result, seen starkly in Figure 4, appears to indicate that CMEs that move faster than the fast solar wind speed remove material so quickly that a short-lived or "transient" coronal hole is truly formed behind the event. Dimmings were originally termed transient coronal holes, and it appears that the physical properties of these regions (as well as the magnetic field topology, e.g., McIntosh et al. 2007) are quite similar to those of longer lived coronal holes.

Rather than velocity alone, it is likely that the determining factor in the dimming creation is the amount of energy in the system. The energy budget available for the event has an impact on the speed of the CME as well as the flare size. Chen et al. (2006) find that both magnetic flux and average magnetic field strength in a filament channel correlate with CME speed. However, we find no significant correlation between magnetic flux in a dimming region and CME speed. One explanation for this lack of correlation is that dimmings often expand beyond and lose their connection with the original source region (Mandrini et al. 2005, 2007; Crooker & Webb 2006; Attrill et al. 2007; Harra et al. 2007); thus, measurements of magnetic flux within the dimming region may have little to no bearing on the flux originally available for the event. On the other hand, the filament, when present, is spatially limited and directly associated with the CME source region and therefore provides a better measurement of the available magnetic flux. Using the Chen et al. (2006) results, and the fact that most of the available energy in the corona is magnetic, it is likely that the discriminator between events that subsequently produce a dimming and those that do not is the energy available in the event.

We propose the following explanation for the dimming association of fast CMEs. The creation of a dimming region on the disk relies on two primary factors. First, the scale height in the corona is about 60,000 km and thus the bulk of coronal mass lies low in the corona (Phillips 1992). Consequently, a depletion must occur low in the corona in order for a dimming to be observed on the disk. We conclude that faster CMEs originate or draw material from low in the corona, perhaps because they are more energetic. Second, in order for a dimming region to be created, plasma must be evacuated from the low corona faster

than it can be replenished. Faster CMEs are therefore more likely to create a dimming. This leads us to focus on a second, more difficult question: *why do some slow CMEs have dimmings?*

In order to look more closely at the difference between dimming and non-dimming events, in the bottom half of Table 1, we separate fast and slow dimming-associated events and compare them to the non-dimming-associated events. We find that, while the fast dimming-associated events have very high flare association and associated flare magnitude, the slow events are nearly identical regardless of whether an associated dimming was present. Therefore, one explanation for these results is a form of the "Big Flare Syndrome" (Kahler 1982). More energy in the system results in more energetic CMEs, larger flares, and associated dimming regions.

As mentioned above, flare association gives some indication of the amount of energy available in the system. We find that the dimming-associated events tend to have a stronger correlation with flare size. In the C-class flare range, the velocities of dimming- and non-dimming-associated events are quite similar. In contrast, for events with an associated M-class flare, those that do not have an associated dimming tend to fall at the lower end of the range of velocities, while nearly all of the dimming-associated events have velocities over 800 km s^{-1}. This result tells us something about the CME/flare energy partition (Emslie et al. 2004). It appears that for non-dimming-associated CMEs, a higher portion of the system energy goes into the production of a flare. The non-dimming-associated CMEs may erupt from higher in the solar atmosphere, thus requiring less energy or the magnetic configuration of the event may affect the partition of energy.

CMEs with dimmings appear at the same longitudes as slow CMEs without dimmings (Figure 3), so we can rule out observational effects having to do with the location on the solar disk. In Figure 5, we do find a solar cycle effect. Non-dimming and dimming events occur at every phase of the solar cycle. Among dimming-associated events, the fast dimmings are much more likely at and following solar minimum, while slow dimmings occur more often on the rising phase of the cycle. From this, we infer a possible observational effect that may cause slow CMEs with and without dimmings. At solar maximum, the overall increased level of activity may make it difficult to see associated dimmings from events with lower energies, while dimmings from similar events observed during solar minimum, when the corona is relatively calm, may be more obvious. Alternatively, there may be more energy present in the corona during solar maximum and the descending phase of the solar cycle.

We also find differences in the active region properties of dimming and non-dimming events. Focusing on the population of events with a slow CME and an associated dimming, we

find that these events tend to have the smallest active region areas, longitudinal extents, and the number of sunspots in the active region. It is surprising that slow CMEs with an associated dimming tend to come from smaller active regions than CMEs without associated dimmings. We find no correlation between active region size and dimming size, so it is unclear why the active region size would have an effect on the existence of a dimming. One possibility is that the active region size is correlated with the solar cycle and thus this measurement is redundant with the results described in the previous paragraph. Alternatively, small active regions, for reasons unknown, may be more likely to produce CMEs that originate low in the corona.

Together, these results may offer insight into CME initiation. These different CME populations may be the result of different CME initiation methods (Klimchuk 2001). For instance, the tether release (Forbes & Isenberg 1991) and or streamer blowout method (Moore & Sterling 2007) could operate in some cases, producing a CME with a maximum velocity of $\sim$800 km s^{-1} and no associated dimming. At other times, the breakout model (Antiochos 1998), for example, could operate, producing a wider variety of speeds and the ability for the CME to open the coronal field to the depths required to cause a dimming.

5. CONCLUSION

In this paper, we compare CME properties with for halo CMEs with and without associated dimmings. We find that CME speed is weakly correlated with dimming size. More strikingly, we find clear differences between the velocities of dimming-associated and non-dimming-associated CMEs. In particular, dimming-associated CMEs tend to occur with a large range of speeds, while CMEs without associated dimmings do not (in our sample) exceed 800 km s^{-1}. In addition, dimming-associated events are more likely to be associated with flares and those flares tend to have the largest magnitudes.

The following scenario summarizes our interpretation of the data. The large amount of energy needed for the expulsion of a fast CME results in more material removed from low in the corona. That material is removed much faster than the filling in time, leaving a large dimming apparent on the solar disk. Once a certain threshold is crossed, fast CMEs always create a dimming, while for slow CMEs the creation of a dimming depends on other factors. These factors may include the initiation height of the CME, the magnetic configuration of the source, and the presence of other activity at the Sun that may obscure the observation of a dimming. A future study, focused on limb dimmings, will address some of these possibilities.

The results summarized in this paper indicate that coronal dimmings have some predictive power beyond indicating whether a halo CME is Earth directed or not. When no dimming is observed, it is likely that the subsequent CME will not exceed 800 km s^{-1}. Conversely, if a dimming is observed, there is more than a 50% likelihood that the CME will be fast. Clearly, more study is needed to extend and clarify these results.

REFERENCES

Antiochos, S. K. 1998, ApJ, 502, L181
Attrill, G. D. R., Harra, L. K., van Driel-Gesztelyi, L., & Demoulin, P. 2007, ApJ, 656, L101
Berger, T. E., de Pontieu, B., Fletcher, L., Schrijver, C. J., Tarbell, T. D., & Title, A. M. 1999, Sol. Phys., 190, 409
Bewsher, D., Harrison, R. A., & Brown, D. S. 2008, A&A, 478, 897
Crooker, N. U., & Webb, D. F. 2006, J. Geophys. Res., 111, A08108
Chen, A. Q., Chen, P. F., & Fang, C. 2006, A&A, 456, 1153
Emslie, A., et al. 2004, J. Geophys. Res., (109: A10104)
Freeland, S. L., & Handy, B. N. 1998, Sol. Phys., 182, 497
Forbes, T. G., & Isenberg, P. A. 1991, ApJ, 373, 294
Gopalswamy, N., & Hanaoka, Y. 1998, ApJ, 498, L179
Hansen, R., Garcia, C., Hansen, S., & Yasukawa, E. 1974, PASP, 86, 500
Harra, L., & Sterling, A. 2001, ApJ, 561, L215
Harra, L. K., et al. 2007, PASJ, 59, S801
Harrison, R., Bryans, P., Simnett, G., & Lyons, M. 2003, A&A, 400, 1071
Harrison, R., & Lyons, M. 2000, A&A, 358, 1097
Howard, R. F., Harvey, J. W., & Forgach, S. 1990, Sol. Phys., 130, 295
Howard, T., Fry, C., Johnston, J., & Webb, D. 2007, ApJ, 667, 610
Hudson, H., Lemen, J., St Cyr, O., Sterling, A., & Webb, D. 1998, Geophys. Res. Lett., 25, 2481
Kahler, S. 1982, J. Geophys. Res., 87, 3439
Klimchuk, J. A. 2001, in Space Weather, Theory of Coronal Mass Ejections, ed. H. J. S. P. Song & G. L. Siscoe (Washington, DC: American Geophysical Union), 143
Mandrini, C. H., Pohjolainen, S., Dasso, S., Green, L. M., Demoulin, P., van Driel-Gesztelyi, L., Copperwheat, C., & Foley, C. 2005, A&A, 434, 725
Mandrini, C. H., Nakwacki, M. S., Attrill, G., van Driel-Gesztelyi, L., Demoulin, P., Dasso, S., & Elliott, H. 2007, Sol. Phys., 244, 25
McIntosh, S., Leamon, R., Davey, A., & Wills-Davey, M. 2007, ApJ, 660, 1653
Moore, R., & Sterling, A. 2007, ApJ, 661, 543
Phillips, K. J. H. 1992, Guide to the Sun (Cambridge: Cambridge Univ. Press)
Press, W. H., Flannery, B. P., Teukolsky, S. A., & Vetterling, W. T. 1989, Numerical Recipes (London: Cambridge Univ. Press)
Qiu, J., Hu, Q., Howard, T., & Yurchyshyn, V. 2007, ApJ, 659, 758
Reinard, A., & Biesecker, D. 2008, ApJ, 674, 576
Richardson, I., & Cane, H. 2008, Near-Earth Interplanetary Coronal Mass Ejections in 1996-2007 (revised May 16, 2008; Pasadena, CA: Caltech) http://www.ssg.sr.unh.edu/mag/ace/ACElists/ICMEtable.html
Rust, D., & Hildner, E. 1976, Solar Physics, 48, 381
Sterling, A., & Hudson, H. 1997, ApJ, 491, L55
Thompson, B., Cliver, E., Nitta, N., Delannee, C., & Delaboudiniere, J. 2000a, Geophys. Res. Lett., 27, 1431
Thompson, B., Cliver, E., Nitta, N., Delannee, C., & Delaboudiniere, J. 2000b, Geophys. Res. Lett., 27, 1865
Thompson, B., et al. 1999, ApJ, 517, L151
Yashiro, S., Gopalswamy, N., Michalek, G., St Cyr, O., Plunkett, S., Rich, N., & Howard, R. 2004, J. Geophys. Res., 109, A07105